

Journal Pre-proof

Efficient removal of Cd(II) from aqueous solution by pinecone biochar: Sorption performance and governing mechanisms

Dongye Teng, Bingbing Zhang, Guomin Xu, Bing Wang, Kang Mao, Jianxu Wang, Jing Sun, Xinbin Feng, Zhugen Yang, Hua Zhang



PII: S0269-7491(20)32318-6

DOI: <https://doi.org/10.1016/j.envpol.2020.115001>

Reference: ENPO 115001

To appear in: *Environmental Pollution*

Received Date: 27 March 2020

Revised Date: 26 May 2020

Accepted Date: 7 June 2020

Please cite this article as: Teng, D., Zhang, B., Xu, G., Wang, B., Mao, K., Wang, J., Sun, J., Feng, X., Yang, Z., Zhang, H., Efficient removal of Cd(II) from aqueous solution by pinecone biochar: Sorption performance and governing mechanisms, *Environmental Pollution* (2020), doi: <https://doi.org/10.1016/j.envpol.2020.115001>.

This is a PDF file of an article that has undergone enhancements after acceptance, such as the addition of a cover page and metadata, and formatting for readability, but it is not yet the definitive version of record. This version will undergo additional copyediting, typesetting and review before it is published in its final form, but we are providing this version to give early visibility of the article. Please note that, during the production process, errors may be discovered which could affect the content, and all legal disclaimers that apply to the journal pertain.

© 2020 Published by Elsevier Ltd.

1 **Efficient Removal of Cd(II) from Aqueous Solution by Pinecone**

2 **Biochar: Sorption Performance and Governing Mechanisms**

3 Dongye Teng^{a,b}, Bingbing Zhang^c, Guomin Xu^c, Bing Wang^{a,d,e}, Kang Mao^a, Jianxu Wang^a, Jing
4 Sun^a, Xinbin Feng^a, Zhugen Yang^f, and Hua Zhang^{a,*}.

5 ^a*State Key Laboratory of Environmental Geochemistry, Institute of Geochemistry, Chinese*

6 *Academy of Sciences, Guiyang, 550081, China*

7 ^b*University of Chinese Academy of Sciences, Beijing 100049, China.*

8 ^c*National Engineering Research Center for Compounding and Modification of Polymer Materials,*

9 *Guiyang, 550014, China*

10 ^d*College of Resource and Environmental Engineering, Guizhou University, Guiyang, 550025,*

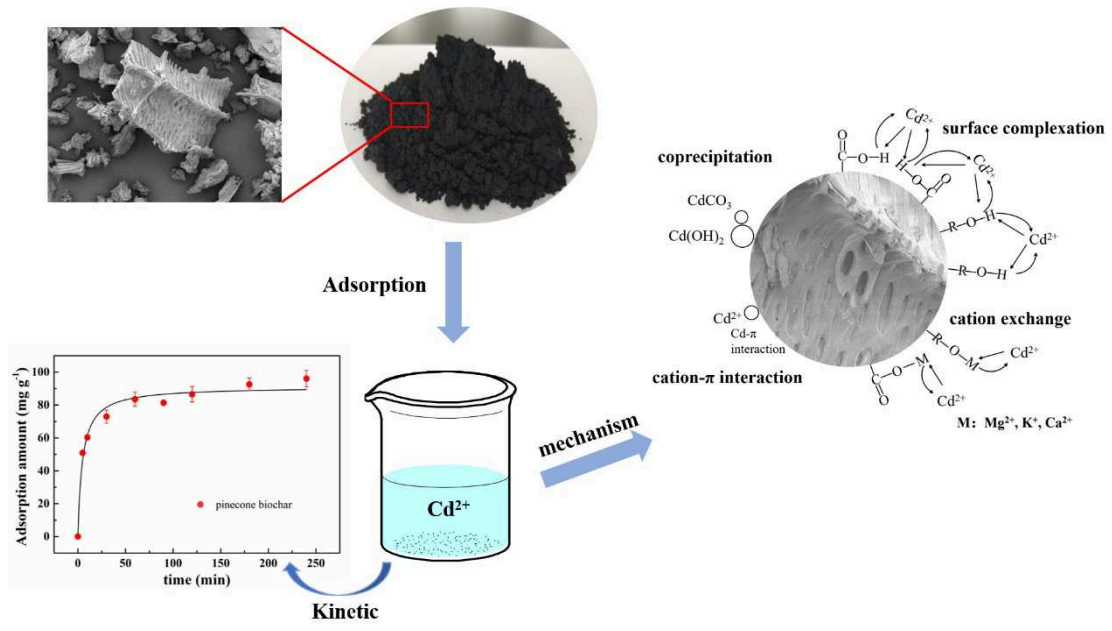
11 *Guizhou, China*

12 ^e*Key Laboratory of Karst Georesources and Environment, Ministry of Education, Guiyang,*

13 *550025, Guizhou, China*

14 ^f*Cranfield Water Science Institute, Cranfield University, Cranfield MK43 0AL, United Kingdom*

15
16
17 Corresponding Email: zhanghua@mail.gyig.ac.cn (Prof. Hua Zhang)
18



19

20

21

Graphic Abstract

22 **Abstract:**

23 Cadmium (Cd) is one of the most harmful and widespread environmental pollutants.
24 Despite decades-long research efforts, the remediation of water contaminated by Cd
25 has remained a significant challenge. A novel carbon material, pinecone biochar, was
26 previously hypothesized to be a promising adsorbent for Cd, while so far, it has
27 received little attention. This study evaluated the sorption capacity of pinecone
28 biochar through isotherm experiments. Based on Langmuir model, the adsorption
29 maximum for Cd(II) was up to 92.7 mg g⁻¹. The mechanism of Cd(II) adsorption on
30 pinecone biochar was also explored through both thermodynamic and kinetics
31 adsorption experiments, as well as both solution and solid-phase microstructure
32 characterization. The solid-solution partitioning behaviour of Cd(II) fitted best with
33 the Tóth model while the adsorption process followed a pseudo-second-order rate,
34 suggesting that the Cd(II) adsorption on the pinecone biochar was mainly a
35 chemisorption process. Microstructure characteristics and mechanism analysis further
36 suggested that coprecipitation and surface complexation were the main mechanisms
37 of Cd adsorption by biochar. Coprecipitation occurred mainly through the forms of
38 Cd(OH)₂ and CdCO₃. Our results demonstrated that pinecone biochar was an efficient
39 adsorbent which holds a huge potential for Cd(II) removal from aqueous solution.

40

41 **Keywords:** Biochar; Cadmium; Adsorption; Heavy metals; Water treatment

42

43 **1. Introduction**

44 In recent years, the discharge of heavy-metal contaminated wastewater from
45 industrial activities has caused serious contamination to soil and aqueous system,
46 posing a great potential threat to human health and aquatic life (Zhang et al., 2019).
47 Especially, due to the higher mobility, long persistence, solubility and biological
48 accumulation of cadmium (Cd), the issue of Cd contamination has caused significant
49 effects on environment and attracted significant concern (Bashir et al., 2018; Liu and
50 Fan, 2018; Peng et al., 2017). Anthropogenic activities such as electroplating, the
51 battery manufacturing industry, mining, smelting processes, alloy manufacturing,
52 manufacturing of phosphate fertilisers, refining of non-ferrous metals and pigments
53 lead to widespread Cd contamination (Ho and Ofomaja, 2006; Moyo et al., 2016;
54 Purkayastha et al., 2014; Zhang et al., 2015), especially in aquatic ecosystems.
55 Moreover, as a carcinogenic toxic heavy metal, Cd can cause a series of diseases
56 including cumulative nephrotoxicity (Jain, 2020). Unlike organic pollutants, Cd is
57 impossible to degrade and shows a half-life of 10-30 years in the kidney (Jarup and
58 Akesson, 2009). Cd contamination has become a serious environmental problem and
59 poses a great threat to human health. Therefore, controlling and removing Cd
60 contamination has aroused widespread concern throughout society.

61 Many physicochemical techniques have been made to control Cd contamination
62 in recent years, such as chemical oxidation, coagulation–precipitation, ion exchange,
63 solvent extraction, electrochemical treatment, reverse osmosis, membrane treatment,
64 and evaporation recovery (Moyo et al., 2016; Purkayastha et al., 2014). However, the
65 traditional process has inherent limitations. For example, ion exchange and reverse
66 osmosis are limited in practical application because of high operation cost (Muya et
67 al., 2016). In comparison, chemical precipitation will create great quantities of Cd
68 sludge (Lodeiro et al., 2006). Recently, biochar has been widely studied owing to its
69 superior chemical stability, excellent adsorption properties, simple operation and low
70 costs (Huang et al., 2019). Biochar is a carbon-rich material with an aromatic
71 structure, high porosity, a large specific surface area and abundant oxygen-containing

72 functional groups (Tan et al., 2016). It is prepared by pyrolysis of biomass under the
73 condition of O₂-limited supply and relatively low temperature (350-700 °C)
74 (Komkiene and Baltrenaite, 2016; Manariotis et al., 2015). Because of its special
75 physicochemical properties, biochar is regarded as a product that can effectively treat
76 Cd contamination in water and soil (Jing et al., 2020). It has been found that biochars
77 produced from different feedstock show diverse adsorption process and mechanisms
78 (Gao et al., 2019; Wang et al., 2018). Numerous studies have investigated the
79 adsorption of Cd by different biochars. For example, Kim et al. (2013) found that the
80 maximum adsorption capacity of Cd by biochar produced from *Miscanthus*
81 *sacchariflorus* at 500 °C was 13.2 mg g⁻¹. The study by Usman et al. (2016) indicates
82 that date palm biochar obtained by pyrolysis at 700 °C shows an Cd adsorption
83 capacity of approximately 43.6 mg g⁻¹. Han et al. (2013) found that the maximum
84 adsorption capacity of Cd by rice straw biochar pyrolyzed at 400 °C was 34.1 mg g⁻¹.
85 In contrast, Bashir et al. (2018) found that the maximum adsorption capacity of Cd by
86 rice straw biochar (produced via pyrolysis at 500 °C) was only 12.2 mg g⁻¹. Based on
87 the above analysis, it is noteworthy that biochars prepared from different raw
88 materials or the same raw materials under different pyrolysis processes show
89 significant differences in adsorption capacities. Indeed, the difference in feedstock and
90 pyrolysis process can alter the surface functional groups, pore structure, elemental
91 composition, and specific surface area of biochar (Wang et al., 2019), leading to
92 dramatically diverse Cd removal efficiencies. Currently, many feedstocks, such as
93 forestry and agricultural residues, domestic garbage, and sludge, can be used as
94 biochar feedstocks. Therefore, experiments on the adsorption properties of biochar
95 prepared from different feedstock are still needed. Moreover, it is urgently necessary
96 to conduct a lot of research on the removal of Cd by biochar.

97 Elemental composition and the contents of cellulose, lignin, hemicellulose in the
98 biochar are affected by the feedstocks, which could regulate the physicochemical
99 properties and ultimately the adsorption characteristics of biochar (Alexis et al., 2007;
100 Brewer et al., 2011; Mimmo et al., 2014). Pinecone, a common litter in the forest,

101 typically consists of 46.5% holocellulose, 37.4% lignin and 18.8% α -cellulose
102 (Ofomaja and Naidoo, 2011). The cellulose, hemicellulose and lignin components
103 provide various functional groups such as alcohols and aldehydes on the surface of
104 pinecone (Van Vinh et al., 2015). According to the results of Igalavithana et al. (2017),
105 the biochar prepared from pinecone at 500 °C has a high surface area of 193 m² g⁻¹.
106 Generally, biochar with large surface area and pore volume can provide abundant
107 adsorption sites for adsorbing pollutants (Park et al., 2016). Therefore, biochar
108 produced from pinecone can potentially be an excellent adsorbent. Dawood et al.
109 (2017) show that the adsorption capacity of pinecone biochar for nickel ions is up to
110 118 mg g⁻¹. Furthermore, pinecone is a cheap feedstock that allows for the sustainable
111 production of economical and environmentally friendly biochar adsorbents (Dawood
112 et al., 2017). There have been many studies on the removal of Cd by biochar prepared
113 from different agricultural and forestry waste as well as animal manure, such as rice
114 straw (Bashir et al., 2018), hickory wood (Wang et al., 2015a) and dairy manure (Xu
115 et al., 2013). The feedstocks for preparing biochar are diverse, but not all of them
116 have the potential to produce an excellent adsorbent. Based on literature (Dawood et
117 al., 2017), we found that the pinecone biochar was an adsorbent worthy of further
118 study. However, to date only sparse information is available on the removal of Cd by
119 pinecone biochar. In this study, pinecone biochar was prepared and selected as an
120 adsorbent to remove Cd from aqueous solution, and then the adsorption equilibrium
121 isotherm and adsorption kinetics were studied. Furthermore, we explored the
122 relationship between the structure and adsorption properties of the prepared pinecone
123 biochar and the adsorption mechanism. In addition, we compared the adsorption
124 capacity of the pinecone biochar used in this study with those of biochars in previous
125 studies.

126 2. Materials and Methods

127 2.1 Materials

128 The pinecone biochar prepared by pyrolysis and carbonization at temperature
129 (350-400 °C) under nitrogen environment was purchased from Shike Jinnian

130 Biotechnology of Guizhou Province (China) Co., Ltd. $\text{CdCl}_2 \cdot 2 \frac{1}{2}\text{H}_2\text{O}$ (greater than
131 99% purity) was purchased from the Science and Technology Development of Tianjin
132 Guangfu Co., Ltd. NaOH (analytical grade) and HNO_3 (ultrapure) were purchased
133 from Sinopharm Chemical Reagent Co., Ltd. All solutions used in this experiment
134 were prepared by using ultrapure water.

135

136 **2.2 Characterization of Pinecone biochar**

137 The morphology and sizes of the pinecone biochar were characterized by
138 scanning electron microscopy (SEM, QUANTA FEG 250, USA) and the element
139 analysis was fulfilled by energy dispersive X-ray spectrometry (EDX).

140 The surface area, pore volume and pore size distribution of the pinecone biochar
141 were detected using a NOVA-1000e automated gas adsorption system (QUANTA,
142 USA) via N_2 adsorption isotherms analysis at 77 K.

143 The surface functional groups of the pinecone biochar were characterized by
144 Fourier transform infrared (FT-IR) spectroscopy in the range of $4000\text{-}400 \text{ cm}^{-1}$. FT-IR
145 were recorded using a NEXUS-670 spectrometer (Thermo Scientific, USA). The
146 sample of pinecone biochar powder was prepared in KBr pressed pellets.

147

148 **2.3 Adsorption Experiments**

149 For adsorption experiments, stock heavy metal solution with a concentration of
150 800 mg L^{-1} was prepared from $\text{CdCl}_2 \cdot 2 \frac{1}{2}\text{H}_2\text{O}$ using ultrapure water and stored in a
151 reagent bottle prior to use.

152 The extent of Cd adsorption can change with pH and Cd concentration.
153 Thermodynamic adsorption experiments as a function of Cd concentration at constant
154 pH (adsorption isotherms) and as a function of pH at constant Cd concentration
155 (adsorption envelopes), therefore, were both conducted. To perform adsorption
156 isotherm experiments, $\text{pH}=6.0$ CdCl_2 solution with initial Cd^{2+} concentration of 10, 30,
157 50, 100, 200, 300, 400 and 600 mg L^{-1} was added into a series of centrifuge tubes, and
158 10 mg biochar was added to each sample. To perform adsorption envelopes, 10 mL of

159 CdCl₂ solution with Cd²⁺ concentration of 200 mg L⁻¹ was placed into a series of 15
160 mL centrifuge tubes, in which 10 mg of biochar was placed. Thereafter, the pH of the
161 suspensions was adjusted to 1, 3, 5, 7, 9, respectively, by using 0.15-1.5M HNO₃ or
162 0.25-2.5M NaOH. Consistent with the procedures in Yang and Jiang (2014) , the pH
163 of suspension of each sample was adjusted after adding biochar.

164 To investigate the influence of adsorption time, 20 mg biochar was added to 20
165 mL CdCl₂ solution (the initial pH of solution was 6.0; the concentration of Cd²⁺ was
166 400 mg L⁻¹) in the centrifuge tubes of 50 ml, and then samples were taken at different
167 time intervals (5, 10, 30, 60, 90, 120, 180, 240 min). All thermodynamic and kinetic
168 adsorption experiments were performed in duplicate at room temperature.

169 Samples were oscillated in a horizontal oscillator at a speed of 250 r min⁻¹ for
170 300 min. After equilibrium, mixtures were centrifuged in a centrifuge at a speed of
171 3000 r min⁻¹ for 25 min. Then, the supernatant of the samples was filtered through a
172 0.45 μm filter and diluted for the determination of Cd. Standard deviations between
173 duplicate experiments were about 5%. Flame atomic absorption spectrometry (AAS,
174 Perkin Elmer, PinAAcle 900F) was used to measure the residual Cd ion content in the
175 solution after adsorption experiments. X-ray photoelectron spectroscopy (XPS) was
176 used to identify the metallic state of element of Cd on the surface of pinecone biochar
177 before and after adsorption. XPS measurements were made with a spectrometer
178 (Thermo Scientific Escalab 250Xi) equipped with a Kα-Al radiation (1486.6 eV, 6
179 mA, 12 kV) as the X-ray source.

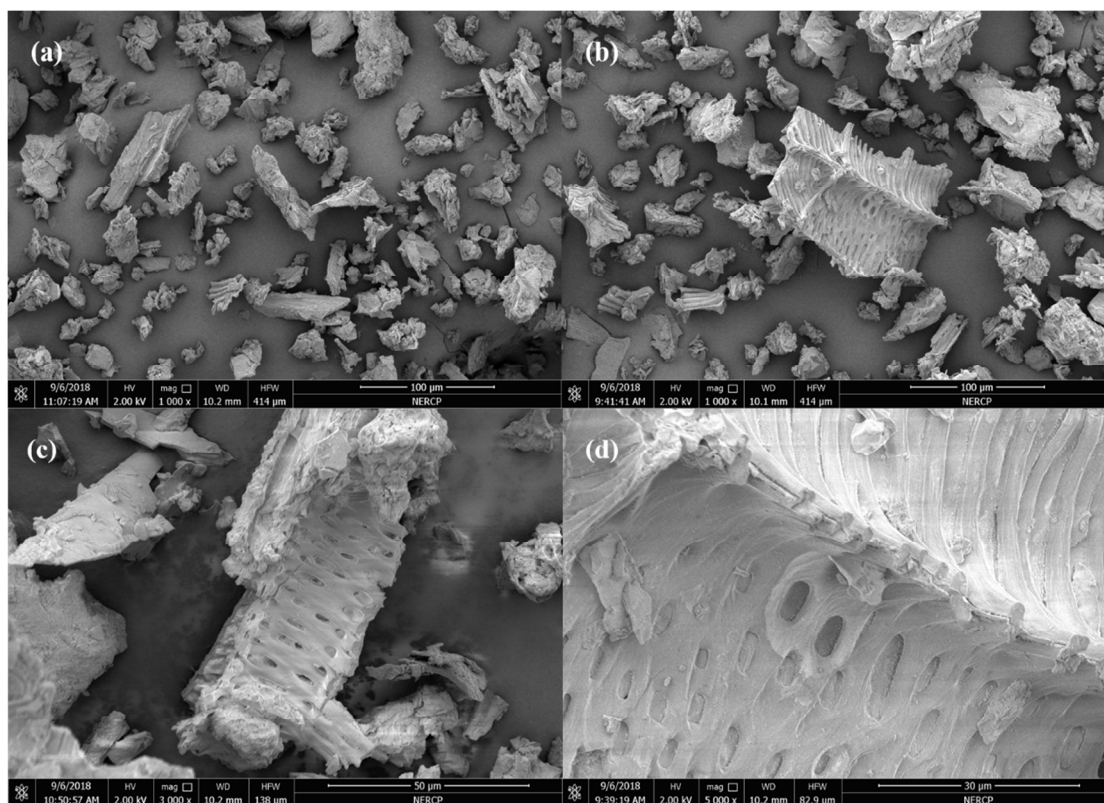
180 Pseudo-first-order kinetic model and pseudo-second-order kinetic model (Eqs.
181 (1)-(4) in supplementary data) were used to investigate the adsorption mechanisms.
182 The Freundlich, Langmuir, Tóth and Langmuir-Freundlich (Sips) models (Eqs. (5)-(8)
183 in supplementary data) were used to investigate the characteristics of adsorption
184 process.

185

3. Results and Discussion

3.1 Characterization of pinecone biochar

Fig. 1 exhibits SEM micro-images of the pinecone biochar with different magnifications of 10^3 x, 3×10^3 x, and 5×10^3 x. The morphology of the pinecone biochar showed a “skeletal structure”, and the particle size was approximately 20-100 μm (as seen in Fig. 1 (a)(b)). Notably, there were many micropores with diameters of approximately 6-10 μm on the surface of the pinecone biochar (as seen in Fig. 1 (c)(d)). Moreover, energy dispersive X-ray spectrometer (EDX) analysis showed that carbon, oxygen and the metallic elements potassium, calcium and magnesium were found on the surface of the pinecone biochar, and the atomic ratio of O/C was approximately 0.36. The FT-IR results indicated that the functional groups of O-H at 3445 cm^{-1} ; C-H at 2925 cm^{-1} and 2854 cm^{-1} ; C=O and C=C at 1634 cm^{-1} ; COOH, CHO, phenolic-OH bending, and CO_3^{2-} at 1458 cm^{-1} ; and C-O at 1113 cm^{-1} were observed on the surface of the pinecone biochar (Fig. S1) (Liu and Fan, 2018; Moyo et al., 2016; Usman et al., 2016; Van Vinh et al., 2015; Yang and Jiang, 2014). From the results of gas adsorption-desorption, the calculated specific surface area, pore volume and pore diameter of the pinecone biochar were $165\text{ m}^2\text{ g}^{-1}$, $0.147\text{ cm}^3\text{ g}^{-1}$ and 15.5 nm, respectively. Amazingly, the specific surface area of the pinecone biochar used in this study was significantly greater than that of materials in previous studies (approximately $19.1\text{ m}^2\text{ g}^{-1}$ for rape straw biochar and $112\text{ m}^2\text{ g}^{-1}$ for wheat straw biochar (Li et al., 2017; Liu and Fan, 2018), which might be attributed to the large number of micropores, as confirmed by the SEM results.



208

209 Fig. 1. SEM micro-images of the pinecone biochar with magnifications of $10^3 \times$, $10^3 \times$, $3 \times 10^3 \times$,
 210 and $5 \times 10^3 \times$.

211

212 3.2 Adsorption performance of Cd(II) by pinecone biochar

213 The effects of solution pH on the Cd^{2+} removal efficiency and adsorption
 214 capacity are shown in Fig. S2. With an increase in pH from 1 to 7, the removal
 215 efficiency of Cd^{2+} increased from 2.39% to 37.5%, and the adsorption capacity of
 216 Cd(II) increased from 5 mg g^{-1} to 74 mg g^{-1} . According to previous studies, the effect
 217 of pH on the removal efficiency and adsorption capacity of Cd(II) by pinecone
 218 biochar is ascribed to three reasons. First of all, under a low-pH environment, the
 219 large amount of H^+ in the system protonates the functional groups on the adsorbent
 220 surface, which results in the rejection of Cd^{2+} in the system (Cheng et al., 2016;
 221 Elaigwu et al., 2014; Liu and Zhang, 2011). Secondly, the adsorption sites on the
 222 adsorbent are limited, and the abundant H^+ in solution competes with Cd^{2+} at the
 223 adsorption sites (Cheng et al., 2016). The higher the H^+ content is, the higher the
 224 probability of adsorption, and the less Cd^{2+} will adsorbed by the adsorbent. Thirdly,

225 metal ions hydrolyse at high pH values, while heavy metals in the form of hydrolytic
 226 species have a higher adsorption density on the surface of biochar (Liao et al., 2016).
 227 Studies have shown that when the pH of solution system reaches 8, a large amount of
 228 OH^- will react with Cd to form several low solubility complexes such as $\text{Cd}(\text{OH})_2$
 229 (Cheng et al., 2016). Therefore, precipitation could be seen at pH of 9 in this study.

230

231 3.3 Adsorption Kinetics

232 The curve of adsorption amount versus adsorption time and the plots of
 233 pseudo-first-order and pseudo-second-order kinetic model are shown in Fig. S3 and
 234 Fig. S4, respectively. Table 1 lists the related parameters obtained according to the
 235 adsorption time experiments and the equations. The adsorption of Cd on pinecone
 236 biochar showed to follow two distinct stages: a rapid adsorption stage during the first
 237 60 min and a slower stage till achieving adsorption equilibrium in approximately 175
 238 min, presumably because of diffusion (Zhang et al., 2018). The adsorption amount at
 239 equilibrium was approximately 96.1 mg g^{-1} (as seen in Fig. S3), and about 87% of the
 240 total adsorption of Cd by pinecone biochar occurred in the first 60 min. The
 241 adsorption process can be divided into bulk transfer, external mass transfer, internal
 242 diffusion and chemical adsorption (Zhang et al., 2019). In this study, the adjusted R^2
 243 of the pseudo-second-order kinetic model (0.996) was higher than that of the
 244 pseudo-first-order kinetic model (0.932), indicating that the Cd^{2+} adsorption process
 245 was fitted by the pseudo-second-order kinetic model and that the adsorption process
 246 was mainly controlled by a chemisorption mechanism (Liu and Fan, 2018). It was
 247 calculated that the adsorption rate was approximately $1.05 \times 10^{-3} \text{ (g mg}^{-1} \text{ min}^{-1})$ and the
 248 theoretical q_e of the pseudo-second-order kinetic model was 97.7 mg g^{-1} , which was
 249 close to the experimental value of 96.1 mg g^{-1} .

250

Table 1 Parameters of kinetic models.

Model	Parameters	
Pseudo-first-order model	$q_e(\text{mg g}^{-1})$	39.7

	$k_1(\times 10^{-3})$ (min^{-1})	13.2
	Adj. R^2	0.932
Pseudo-second-order model	$q_e(\text{mg g}^{-1})$	97.7
	$k_2(\times 10^{-3})$ ($\text{g mg}^{-1} \text{min}^{-1}$)	1.05
	Adj. R^2	0.996
	Experiment	$q_e(\text{mg g}^{-1})$

251

252 **3.4 Adsorption equilibrium isotherms**

253 The adsorption isotherms of Freundlich, Langmuir, Tóth and
254 Langmuir-Freundlich plotted against initial concentrations of Cd^{2+} solution from 10 to
255 600 mg L^{-1} are shown in Fig. S5, and the regression parameters are listed in Table 2.
256 Fig. S5 shows that the equilibrium adsorption capacity of Cd^{2+} ions increased quickly
257 with an increasing concentration of Cd^{2+} ions in the initial stage (lower concentration)
258 and then slowed until reaching equilibrium. The adsorption capacity of pinecone
259 biochar for Cd in this study was estimated by the Langmuir model to be 92.7 mg g^{-1} .
260 The correlation coefficient (Adj. R^2) of the Tóth isotherm model (0.973) was higher
261 than those of the Langmuir isotherm model (0.964) and Freundlich isotherm model
262 (0.935). The non-linear regression coefficients (Adj. R^2) of the Tóth model (0.973)
263 and Langmuir-Freundlich model (0.972) were similar, while the Tóth isotherm had a
264 slightly higher Adj. R^2 than the Langmuir-Freundlich isotherm. Moreover, among the
265 four models, the residual sum of squares (RSS) and Chi-squares (χ^2) of the Tóth
266 isotherm were the lowest, which were 143 and 28.6, respectively (Table S1). All the
267 goodness of fit indexes indicated that the Tóth model fitted the adsorption data better
268 than the other isotherm models. The parameter m of Tóth model was 0.499, which
269 deviated from unity. These results showed that the adsorption of Cd^{2+} by pinecone
270 biochar was heterogeneous. In addition, the n_{LF} of the Langmuir-Freundlich model
271 was 0.668, which was less than 1, further indicating that the surface of the adsorbent

272 was heterogeneous. This result was supported by SEM results, which also showed the
 273 surface to be heterogenous. The Langmuir-Freundlich isotherm model showed that the
 274 adsorption of Cd^{2+} by pinecone biochar was controlled by diffusion and saturated
 275 monolayer adsorption at low and high concentrations, respectively (Mohan et al.,
 276 2014; Mohan et al., 2011).

277 It is known that the separation factor R_L can be used to further describe the basic
 278 characteristics of the Langmuir model: when $R_L > 1$, adsorption is unfavourable; when
 279 $0 < R_L < 1$, adsorption is favourable; when $R_L = 1$, adsorption is linear; and when R_L
 280 $= 0$, adsorption is nonlinear (Hall et al., 1966; Reguyal et al., 2017). The R_L has a
 281 negative correlation with the initial concentration of Cd in solution, which is
 282 calculated by substituting the parameter K_L of the Langmuir model into the equation
 283 $R_L = 1/(1+K_L C_0)$, where C_0 is the initial concentration of solution (Cheng et al., 2016;
 284 Reguyal et al., 2017). In this experiment, the calculated value of R_L was from 0.027 to
 285 0.625, further signifying that there was great affinity between Cd and pinecone
 286 biochar and that the adsorption process was favourable. In addition, an adsorption
 287 system can be characterized by the exponent n of the Freundlich model (Zhou et al.,
 288 2018). A value of $1/n$ in the range of 0-1 indicates that adsorption is favourable. In this
 289 study, the value of $1/n$ for Cd was 0.264, further confirming that the adsorption
 290 process was favourable.

291

Table 2 Cd adsorption isotherm parameters determined using the Freundlich,
 Langmuir, Tóth and Langmuir-Freundlich models.

Model	Parameters
Freundlich	$1/n$ 0.264
	$K_F (\text{mg}^{1-1/n} \text{g}^{-1} \text{L}^{1/n})$ 19.8
	Adj. R^2 0.935
Langmuir	$q_{\text{max}} (\text{mg g}^{-1})$ 92.7
	$K_L (\text{L mg}^{-1})$ 0.060

	Adj. R ²	0.964
Tóth	q_{\max} (mg g ⁻¹)	117
	K_T (L mg ⁻¹)	0.158
	m	0.499
	Adj. R ²	0.973
Langmuir-Freundlich	a_{LF} (L mg ⁻¹)	0.107
	K_{LF} (L g ⁻¹)	11.6
	n_{LF}	0.668
	Adj. R ²	0.972

292

293 Recently, many studies have been carried out to explore the Cd removing
 294 efficiency of biochar prepared from different feedstocks. The theoretical maximum
 295 adsorption capacities (q_{\max}) of biochars prepared from different raw materials reported
 296 in previous studies were compared in Table S2. Excitingly, the q_{\max} of the pinecone
 297 biochar used in this study (approximately 92.7 mg g⁻¹) was much higher than those
 298 common biochars reported in previous studies, such as straw, peanut husk and
 299 ipomoea biochar. The results of Cui et al. (2016b) show that the adsorption capacity
 300 of biochar prepared by wetland-plants reaches 119-126 mg g⁻¹, which is better than
 301 that of biochar produced from pinecone. However, pinecone biomass, as a low-cost
 302 and easily available biomass, was also an excellent feedstock of preparing biochars.

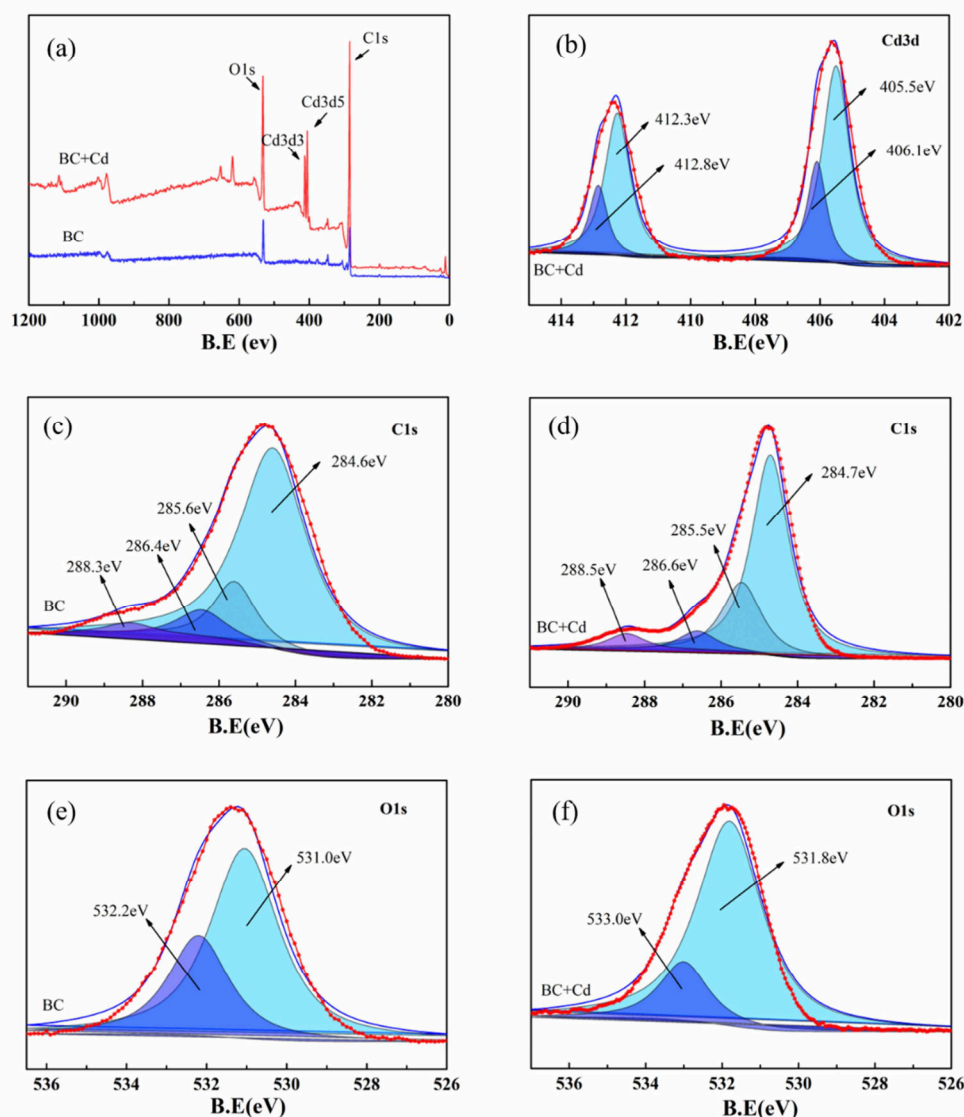
303

304 **3.5 Cd adsorption mechanism**

305 Based on the structural analysis results, it was apparent that the surface
 306 functional groups of the pinecone biochar used in this study were abundant, implying
 307 that many heavy metal chemisorption sites existed on the surface of the pinecone
 308 biochar and were responsible for the excellent adsorption performance of the pinecone
 309 biochar. Moreover, from the results of the isothermal adsorption model, diffusion was
 310 another means of Cd²⁺ adsorption; as a result, the specific surface area also
 311 contributed to the improvement of adsorption performance. Thus, it was inferred that

312 the synergistic effect of the abundant functional groups and the relatively large
313 specific surface area led to the superior adsorption performance of Cd^{2+} by the
314 pinecone biochar in this study.

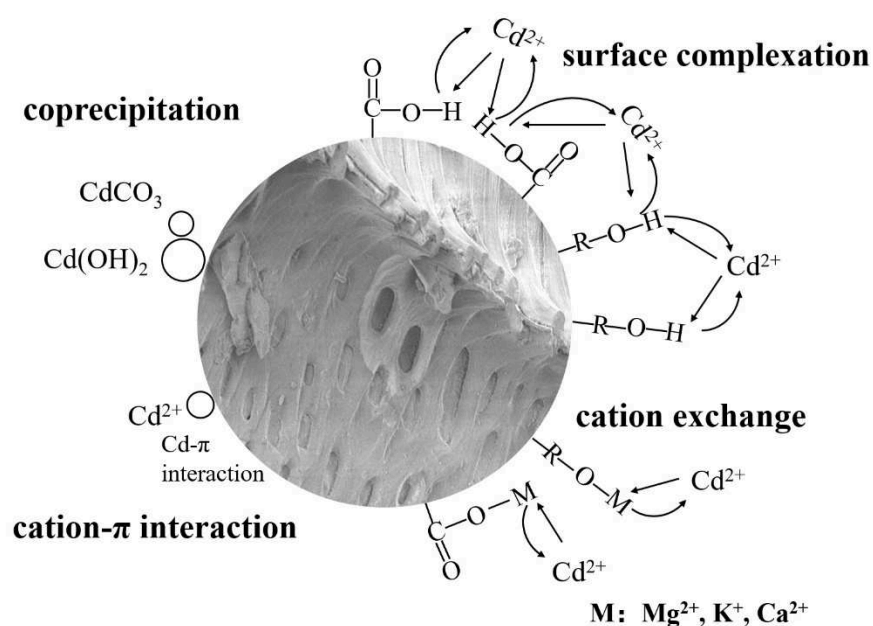
315 To further explore the fixing mechanism of Cd ions onto the surface of the
316 pinecone biochar at the micro level, XPS analysis was also carried out. Fig. 2 shows
317 XPS spectra of the pinecone biochar before and after adsorption of Cd^{2+} . Cd3d peaks
318 appeared in the XPS spectra after adsorption of Cd^{2+} (see Fig. 2 (a)), further
319 indicating that Cd ions were adsorbed on the surface of the pinecone biochar. From
320 the high-resolution XPS spectra of Cd3d, as shown in Fig. 2 (b), Cd ions were bound
321 on the pinecone biochar by CdCO_3 bonds, as confirmed by the strong peaks at 405.5
322 eV, as well as $\text{Cd}(\text{OH})_2$ bonds, corresponding to peaks at 406.1 eV. The peak at 405.5
323 eV also suggested that Cd was adsorbed by biochar through complexation with
324 hydroxyl (-OH) or deprotonated form (O^-) (Zhang et al., 2015). The high-resolution
325 XPS spectrum of C1s of the biochar before the adsorption of Cd ions is shown in Fig.
326 2 (c). The peaks at 284.6 eV, 285.6 eV, 286.4 eV and 288.3 eV were attributed to
327 C-C/C-H, C-O, C=O/C-O-C and O=C-O (bound to carboxyl and/or ester groups),
328 respectively (Jing et al., 2014; Liu and Fan, 2018). As shown in Fig. 2 (d), the
329 high-resolution XPS spectrum of C1s after Cd adsorption also exhibits four peaks
330 similar to those before Cd adsorption, indicating that C atoms did not react with Cd
331 ions (Li et al., 2016). Comparing the results of Fig. 2 (e) and (f) showed that the two
332 major O1s peaks at 531.0 eV and 532.2 eV have a small shift to 531.8 eV and 533.0
333 eV, respectively. The change of O1s after Cd adsorption suggested that Cd was bound
334 to the oxygen-containing functional groups of biochar (Liu and Fan, 2018).



335
 336 Fig. 2. XPS spectra of pinecone biochar loaded with Cd (a) and high-resolution XPS spectra of the
 337 related elements (b-f).

338 Previous studies show that there are four main mechanism for Cd adsorption by
 339 biochar: 1) coprecipitation; 2) metal ion exchange; 3) surface complexation; 4) Cd- π
 340 interaction (Cui et al., 2016a). The adsorption process and mechanism of Cd(II) on the
 341 pinecone biochar were revealed and were illustrated in the schematic drawing in Fig.
 342 3. The high-resolution XPS spectra of Cd3d suggested some anions co-precipitated
 343 with Cd^{2+} and formed $\text{Cd}(\text{OH})_2$ and CdCO_3 minerals on the surface of the pinecone
 344 biochar. The complexation of oxygen-containing functional groups on the surface of
 345 biochar with metal ions is one of the main mechanisms for biochar to adsorb metals

346 (Cui et al., 2016a). From the results of FT-IR, it was known that the surface of the
 347 pinecone biochar contained oxygen-containing functional groups such as -OH and
 348 -COOH. And the XPS analysis of O1s further proved that the coordination between
 349 Cd^{2+} and oxygen-containing functional groups. Ion exchange is considered to be a
 350 common mechanism for the adsorption of metal ions on biochar (Gao et al., 2019; Li
 351 et al., 2013). Metal ions Mg^{2+} , K^+ , Ca^{2+} were detected on pinecone biochar by energy
 352 dispersive X-ray spectrometer (EDX). Therefore, we speculated that a weak ion
 353 exchange occurred during the adsorption of Cd by pinecone biochar. Cation- π
 354 interaction is a noncovalent interaction between a cation and a π -donor (Keiluweit and
 355 Kleber, 2009). The π -system serves as the π -donor and the ability of aromatic
 356 π -system to provide electrons increases with the number of corresponding rings
 357 (Wang et al., 2015b). FT-IR showed that the pinecone biochar contained aromatic
 358 C=C and C=O which could provide π -donor. Thus, we concluded that the Cd- π
 359 interaction occurs in pinecone biochar. By comprehensive comparison, we believed
 360 that coprecipitation and surface complexation were the main mechanisms for Cd
 361 adsorption by pinecone biochar. In contrast, cation- π interaction and ion exchange
 362 were relatively insignificant.



363

364

Fig. 3. Adsorption process and mechanism of Cd(II) on pinecone biochar.

365 **4. Conclusions**

366 In this study, we explored a novel pinecone biochar with a high Cd(II) adsorption
367 capacity of 92.7 mg g⁻¹ and studied the adsorption equilibrium isotherm and
368 adsorption kinetics of the pinecone biochar. The experimental adsorption isotherm
369 results indicated that the adsorption behaviour of Cd(II) onto the pinecone biochar
370 fitted the Tóth model, signifying that there was great affinity between Cd(II) and
371 pinecone biochar, the adsorption process was favourable, and the adsorption
372 behaviour was highly heterogeneous. The adsorption kinetics showed that the
373 adsorption process of Cd(II) by the pinecone biochar fitted the pseudo-second-order
374 kinetic model and that the adsorption process was mainly controlled by a
375 chemisorption. And the main mechanisms of Cd adsorption were coprecipitation and
376 surface complexation. The detailed analysis demonstrated that coprecipitation
377 occurred mainly through Cd(OH)₂ and CdCO₃. We believe that the prepared pinecone
378 biochar was an economical and effective adsorbent for Cd and had a huge potential to
379 remove heavy metal contamination in aqueous solution. We are exploring the
380 potential for testing the real sample and scaling up in the field to evidence the impact
381 for effective remediation.

Acknowledgements

The authors would like to acknowledge the financially supported from Financial support from National Key Research and Development Program of China (No. 2019 YFC1803600), the National Science Foundation of China-Project of Karst Science Research Center (U1612442), and Science and Technology Program of Guizhou Province [Grant No. (2019)5618, 2019(2963), (2019)2836, and (2019)4428]. ZY thanks UK NERC Fellowship grant (NE/R013349/2) and Royal Academy of Engineering Frontier Follow-up Grant (FF\1920\1\36).

390

391

392

References:

- 393 Alexis, M.A., Rasse, D.P., Rumpel, C., Bardoux, G., Péchot, N., Schmalzer, P., Drake, B., Mariotti, A.,
 394 2007. Fire impact on C and N losses and charcoal production in a scrub oak ecosystem.
 395 *Biogeochemistry* 82, 201-216.
- 396 Bashir, S., Zhu, J., Fu, Q., Hu, H., 2018. Comparing the adsorption mechanism of Cd by rice straw
 397 pristine and KOH-modified biochar. *Environ. Sci. Pollut. Res.* 25, 11875-11883.
- 398 Brewer, C.E., Unger, R., Schmidt-Rohr, K., Brown, R.C., 2011. Criteria to Select Biochars for Field
 399 Studies based on Biochar Chemical Properties. *BioEnergy Research* 4, 312-323.
- 400 Cheng, Q., Huang, Q., Khan, S., Liu, Y., Liao, Z., Li, G., Ok, Y.S., 2016. Adsorption of Cd by peanut
 401 husks and peanut husk biochar from aqueous solutions. *Ecol. Eng.* 87, 240-245.
- 402 Cui, X., Fang, S., Yao, Y., Li, T., Ni, Q., Yang, X., He, Z., 2016a. Potential mechanisms of cadmium
 403 removal from aqueous solution by *Canna indica* derived biochar. *Sci. Total Environ.* 562, 517-525.
- 404 Cui, X., Hao, H., Zhang, C., He, Z., Yang, X., 2016b. Capacity and mechanisms of ammonium and
 405 cadmium sorption on different wetland-plant derived biochars. *Sci. Total Environ.* 539, 566-575.
- 406 Dawood, S., Sen, T.K., Phan, C., 2017. Synthesis and characterization of slow pyrolysis pine cone
 407 bio-char in the removal of organic and inorganic pollutants from aqueous solution by adsorption:
 408 Kinetic, equilibrium, mechanism and thermodynamic. *Bioresour. Technol.* 246, 76-81.
- 409 Elaigwu, S.E., Rocher, V., Kyriakou, G., Greenway, G.M., 2014. Removal of Pb²⁺ and Cd²⁺ from
 410 aqueous solution using chars from pyrolysis and microwave-assisted hydrothermal carbonization
 411 of *Prosopis africana* shell. *J. Ind. Eng. Chem.* 20, 3467-3473.
- 412 Gao, L.Y., Deng, J.H., Huang, G.F., Li, K., Cai, K.Z., Liu, Y., Huang, F., 2019. Relative distribution of
 413 Cd²⁺ adsorption mechanisms on biochars derived from rice straw and sewage sludge. *Bioresour.*
 414 *Technol.* 272, 114-122.
- 415 Hall, K.R., Eagleton, L.C., Acrivos, A., Vermeulen, T., 1966. PORE- AND SOLID-DIFFUSION
 416 KINETICS IN FIXED-BED ADSORPTION UNDER CONSTANT-PATTERN CONDITIONS.
 417 *Ind. Eng. Chem. Fundam.* 5, 212-+.
- 418 Han, X., Liang, C.F., Li, T.Q., Wang, K., Huang, H.G., Yang, X.E., 2013. Simultaneous removal of
 419 cadmium and sulfamethoxazole from aqueous solution by rice straw biochar. *J. Zhejiang Univ.-Sci.*
 420 *B* 14, 640-649.
- 421 Ho, Y.S., Ofomaja, A.E., 2006. Biosorption thermodynamics of cadmium on coconut copra meal as
 422 biosorbent. *Biochem. Eng. J.* 30, 117-123.
- 423 Huang, Y., Xia, S., Lyu, J., Tang, J., 2019. Highly efficient removal of aqueous Hg²⁺ and CH₃Hg⁺ by
 424 selective modification of biochar with 3-mercaptopropyltrimethoxysilane. *Chem. Eng. J.* 360,
 425 1646-1655.
- 426 Igalavithana, A.D., Lee, S.-E., Lee, Y.H., Tsang, D.C.W., Rinklebe, J.r., Kwon, E.E., Ok, Y.S., 2017.
 427 Heavy metal immobilization and microbial community abundance by vegetable waste and pine
 428 cone biochar of agricultural soils. *Chemosphere* 174, 593-603.
- 429 Jain, R.B., 2020. Cadmium and kidney function: Concentrations, variabilities, and associations across
 430 various stages of glomerular function. *Environ. Pollut.* 256.
- 431 Jarup, L., Akesson, A., 2009. Current status of cadmium as an environmental health problem. *Toxicol.*
 432 *Appl. Pharmacol.* 238, 201-208.
- 433 Jing, F., Chen, C., Chen, X., Liu, W., Wen, X., Hu, S., Yang, Z., Guo, B., Xu, Y., Yu, Q., 2020. Effects
 434 of wheat straw derived biochar on cadmium availability in a paddy soil and its accumulation in

- 435 rice. *Environ. Pollut.* 257.
- 436 Jing, X.R., Wang, Y.-Y., Liu, W.-J., Wang, Y.-K., Jiang, H., 2014. Enhanced adsorption performance of
437 tetracycline in aqueous solutions by methanol-modified biochar. *Chem. Eng. J.* 248, 168-174.
- 438 Keiluweit, M., Kleber, M., 2009. Molecular-Level Interactions in Soils and Sediments: The Role of
439 Aromatic π -Systems. *Environ. Sci. Technol.* 43, 3421-3429.
- 440 Kim, W.-K., Shim, T., Kim, Y.-S., Hyun, S., Ryu, C., Park, Y.-K., Jung, J., 2013. Characterization of
441 cadmium removal from aqueous solution by biochar produced from a giant *Miscanthus* at different
442 pyrolytic temperatures. *Bioresour. Technol.* 138, 266-270.
- 443 Komkiene, J., Baltreinaite, E., 2016. Biochar as adsorbent for removal of heavy metal ions Cadmium(II),
444 Copper(II), Lead(II), Zinc(II) from aqueous phase. *Int. J. Environ. Sci. Technol.* 13, 471-482.
- 445 Li, B., Yang, L., Wang, C.-q., Zhang, Q.-p., Liu, Q.-c., Li, Y.-d., Xiao, R., 2017. Adsorption of Cd(II)
446 from aqueous solutions by rape straw biochar derived from different modification processes.
447 *Chemosphere* 175, 332-340.
- 448 Li, M., Liu, Q., Guo, L., Zhang, Y., Lou, Z., Wang, Y., Qian, G., 2013. Cu(II) removal from aqueous
449 solution by *Spartina alterniflora* derived biochar. *Bioresour. Technol.* 141, 83-88.
- 450 Li, M., Zhang, Z., Li, R., Wang, J.J., Ali, A., 2016. Removal of Pb(II) and Cd(II) ions from aqueous
451 solution by thiosemicarbazide modified chitosan. *Int. J. Biol. Macromol.* 86, 876-884.
- 452 Liao, I.H., Huang, J.-H., Wang, S.-L., Cheng, M.-P., Liu, J.-C., 2016. Adsorptions of Cd(II) and Pb(II)
453 in aqueous solution by rice-straw char. *Desalin. Water Treat.* 57, 21619-21626.
- 454 Liu, L., Fan, S., 2018. Removal of cadmium in aqueous solution using wheat straw biochar: effect of
455 minerals and mechanism. *Environ. Sci. Pollut. Res.* 25, 8688-8700.
- 456 Liu, Z., Zhang, F.-S., 2011. Removal of copper (II) and phenol from aqueous solution using porous
457 carbons derived from hydrothermal chars. *Desalination* 267, 101-106.
- 458 Lodeiro, P., Herrero, R., Sastre de Vicente, M.E., 2006. Thermodynamic and kinetic aspects on the
459 biosorption of cadmium by low cost materials: A review. *Environ. Chem.* 3, 400-418.
- 460 Manariotis, I.D., Fotopoulou, K.N., Karapanagioti, H.K., 2015. Preparation and Characterization of
461 Biochar Sorbents Produced from Malt Spent Rootlets. *Ind. Eng. Chem. Res.* 54, 9577-9584.
- 462 Mimmo, T., Panzacchi, P., Baratieri, M., Davies, C.A., Tonon, G., 2014. Effect of pyrolysis temperature
463 on miscanthus (*Miscanthus × giganteus*) biochar physical, chemical and functional properties.
464 *Biomass Bioenergy* 62, 149-157.
- 465 Mohan, D., Kumar, H., Sarswat, A., Alexandre-Franco, M., Pittman, C.U., Jr., 2014. Cadmium and lead
466 remediation using magnetic oak wood and oak bark fast pyrolysis bio-chars. *Chem. Eng. J.* 236,
467 513-528.
- 468 Mohan, D., Rajput, S., Singh, V.K., Steele, P.H., Pittman, C.U., Jr., 2011. Modeling and evaluation of
469 chromium remediation from water using low cost bio-char, a green adsorbent. *J. Hazard. Mater.*
470 188, 319-333.
- 471 Moyo, M., Lindiwe, S.T., Sebata, E., Nyamunda, B.C., Guyo, U., 2016. Equilibrium, kinetic, and
472 thermodynamic studies on biosorption of Cd(II) from aqueous solution by biochar. *Res.Chem.*
473 *Intermed.* 42, 1349-1362.
- 474 Muya, F.N., Sunday, C.E., Baker, P., Iwuoha, E., 2016. Environmental remediation of heavy metal ions
475 from aqueous solution through hydrogel adsorption: a critical review. *Water Sci. Technol.* 73,
476 983-992.
- 477 Ofomaja, A.E., Naidoo, E.B., 2011. Biosorption of copper from aqueous solution by chemically
478 activated pine cone: A kinetic study. *Chem. Eng. J.* 175, 260-270.

- 479 Park, J.-H., Ok, Y.S., Kim, S.-H., Cho, J.-S., Heo, J.-S., Delaune, R.D., Seo, D.-C., 2016. Competitive
480 adsorption of heavy metals onto sesame straw biochar in aqueous solutions. *Chemosphere* 142,
481 77-83.
- 482 Peng, H., Gao, P., Chu, G., Pan, B., Peng, J., Xing, B., 2017. Enhanced adsorption of Cu(II) and Cd(II)
483 by phosphoric acid-modified biochars. *Environ. Pollut.* 229, 846-853.
- 484 Purkayastha, D., Mishra, U., Biswas, S., 2014. A comprehensive review on Cd(II) removal from
485 aqueous solution. *J. Water Process Eng.* 2, 105-128.
- 486 Reguyal, F., Sarmah, A.K., Gao, W., 2017. Synthesis of magnetic biochar from pine sawdust via
487 oxidative hydrolysis of FeCl₂ for the removal sulfamethoxazole from aqueous solution. *J. Hazard.*
488 *Mater.* 321, 868-878.
- 489 Tan, G., Sun, W., Xu, Y., Wang, H., Xu, N., 2016. Sorption of mercury (II) and atrazine by biochar,
490 modified biochars and biochar based activated carbon in aqueous solution. *Bioresour. Technol.*
491 211, 727-735.
- 492 Usman, A., Sallam, A., Zhang, M., Vithanage, M., Ahmad, M., Al-Farraj, A., Ok, Y.S., Abduljabbar, A.,
493 Al-Wabel, M., 2016. Sorption Process of Date Palm Biochar for Aqueous Cd (II) Removal:
494 Efficiency and Mechanisms. *Water, Air, Soil, Pollut.* 227.
- 495 Van Vinh, N., Zafar, M., Behera, S.K., Park, H.S., 2015. Arsenic(III) removal from aqueous solution by
496 raw and zinc-loaded pine cone biochar: equilibrium, kinetics, and thermodynamics studies. *Int. J.*
497 *Environ. Sci. Technol.* 12, 1283-1294.
- 498 Wang, H., Gao, B., Wang, S., Fang, J., Xue, Y., Yang, K., 2015a. Removal of Pb(II), Cu(II), and Cd(II)
499 from aqueous solutions by biochar derived from KMnO₄ treated hickory wood. *Bioresour.*
500 *Technol.* 197, 356-362.
- 501 Wang, R.Z., Huang, D.L., Liu, Y.G., Zhang, C., Lai, C., Zeng, G.M., Cheng, M., Gong, X.M., Wan, J.,
502 Luo, H., 2018. Investigating the adsorption behavior and the relative distribution of Cd²⁺ sorption
503 mechanisms on biochars by different feedstock. *Bioresour. Technol.* 261, 265-271.
- 504 Wang, Y., Dong, H., Li, L., Tian, R., Chen, J., Ning, Q., Wang, B., Tang, L., Zeng, G., 2019. Influence
505 of feedstocks and modification methods on biochar's capacity to activate hydrogen peroxide for
506 tetracycline removal. *Bioresour. Technol.* 291.
- 507 Wang, Z., Liu, G., Zheng, H., Li, F., Ngo, H.H., Guo, W., Liu, C., Chen, L., Xing, B., 2015b.
508 Investigating the mechanisms of biochar's removal of lead from solution. *Bioresour. Technol.* 177,
509 308-317.
- 510 Xu, X., Cao, X., Zhao, L., Wang, H., Yu, H., Gao, B., 2013. Removal of Cu, Zn, and Cd from aqueous
511 solutions by the dairy manure-derived biochar. *Environ. Sci. Pollut. Res.* 20, 358-368.
- 512 Yang, G.X., Jiang, H., 2014. Amino modification of biochar for enhanced adsorption of copper ions
513 from synthetic wastewater. *Water Res.* 48, 396-405.
- 514 Zhang, F., Wang, X., Yin, D., Peng, B., Tan, C., Liu, Y., Tan, X., Wu, S., 2015. Efficiency and
515 mechanisms of Cd removal from aqueous solution by biochar derived from water hyacinth
516 (*Eichornia crassipes*). *J. Environ. Manage.* 153, 68-73.
- 517 Zhang, H., Yue, X., Li, F., Xiao, R., Zhang, Y., Gu, D., 2018. Preparation of rice straw-derived biochar
518 for efficient cadmium removal by modification of oxygen-containing functional groups. *Sci. Total*
519 *Environ.* 631-632, 795-802.
- 520 Zhang, Z., He, S., Zhang, Y., Zhang, K., Wang, J., Jing, R., Yang, X., Hu, Z., Lin, X., Li, Y., 2019.
521 Spectroscopic investigation of Cu²⁺, Pb²⁺ and Cd²⁺ adsorption behaviors by chitosan-coated
522 argillaceous limestone: Competition and mechanisms. *Environ. Pollut.* 254.

523 Zhou, Q., Liao, B., Lin, L., Qiu, W., Song, Z., 2018. Adsorption of Cu(II) and Cd(II) from aqueous
524 solutions by ferromanganese binary oxide-biochar composites. *Sci. Total Environ.* 615, 115-122.
525

Journal Pre-proof

Highlights

- The amount of Cd^{2+} adsorbed by pinecone biochar increased with the increase of pH.
- The adsorption behavior of Cd(II) onto the pinecone biochar fitted the Tóth model.
- The adsorption process was mainly controlled by a chemisorption mechanism.
- The adsorption capacity of the pinecone biochar was excellent.
- Pinecone was a potential raw material for biochar preparation.

Dongye Teng: Conceptualization, Methodology, Software, Data curation, Writing- Original draft preparation. **Bingbing Zhang:** Conceptualization, Methodology. **Bing Wang:** Writing- Reviewing and Editing. **Kang Mao:** Writing- Reviewing and Editing. **Jianxu Wang:** Writing- Reviewing and Editing. **Jing Sun:** Writing- Reviewing and Editing. **Xinbin Feng:** Writing- Reviewing and Editing. **Zhugen Yang:** Writing- Reviewing and Editing. **Hua Zhang:** Supervision, Conceptualization, Methodology, Writing- Reviewing and Editing.

The authors declare no competing financial interest.

Journal Pre-proof